

Journal Pre-proof

Orthogonal techniques to study the effect of pH, sucrose and arginine salts on monoclonal antibody physical stability and aggregation during long-term storage

Hristo L. Svilenov, Alina Kulakova, Matja Zalar, Alexander P. Golovanov, Pernille Harris, Gerhard Winter

PII: S0022-3549(19)30737-3

DOI: <https://doi.org/10.1016/j.xphs.2019.10.065>

Reference: XPHS 1792

To appear in: *Journal of Pharmaceutical Sciences*

Received Date: 14 August 2019

Revised Date: 14 October 2019

Accepted Date: 31 October 2019

Please cite this article as: Svilenov HL, Kulakova A, Zalar M, Golovanov AP, Harris P, Winter G, Orthogonal techniques to study the effect of pH, sucrose and arginine salts on monoclonal antibody physical stability and aggregation during long-term storage, *Journal of Pharmaceutical Sciences* (2019), doi: <https://doi.org/10.1016/j.xphs.2019.10.065>.

This is a PDF file of an article that has undergone enhancements after acceptance, such as the addition of a cover page and metadata, and formatting for readability, but it is not yet the definitive version of record. This version will undergo additional copyediting, typesetting and review before it is published in its final form, but we are providing this version to give early visibility of the article. Please note that, during the production process, errors may be discovered which could affect the content, and all legal disclaimers that apply to the journal pertain.

© 2019 Published by Elsevier Inc. on behalf of the American Pharmacists Association.



Orthogonal techniques to study the effect of pH, sucrose and arginine salts on monoclonal antibody physical stability and aggregation during long-term storage

Hristo L. Svilenov^{1*}, Alina Kulakova², Matja Zalar³, Alexander P. Golovanov³, Pernille Harris²
and Gerhard Winter¹

¹ Department of Pharmacy, Pharmaceutical Technology and Biopharmaceutics, Ludwig-Maximilians-University, Butenandtstrasse 5-13, Munich D-81377, Germany

² Technical University of Denmark, Department of Chemistry, Kemitorvet 207, 2800 Kongens Lyngby, Denmark

³ Manchester Institute of Biotechnology and Department of Chemistry, Faculty of Science and Engineering, The University of Manchester, 131 Princess Street, Manchester, M1 7DN, UK

*Corresponding author:

Hristo L. Svilenov

Email: hrisph@cup.uni-muenchen.de

ORCID: <https://orcid.org/0000-0001-5863-9569>

KEYWORDS: Monoclonal antibody(s), pH, Sucrose, Arginine, Physical stability, Protein aggregation, Protein formulation, Fluorescence spectroscopy, Light scattering (dynamic), Nuclear Magnetic Resonance (NMR) spectroscopy

ABBREVIATIONS:

A_2 - second virial coefficient

ACF – autocorrelation function

AF^{STD} - protein-additive saturation transfer difference amplification factors from NMR

D - mutual diffusion coefficient from DLS

DLS - dynamic light scattering

D_{max} – maximum dimension from SAXS

FI350/FI330 – intrinsic protein fluorescence intensity ratio 350nm/330nm

IP1 - inflection point of the first thermal unfolding (at a lower temperature)

IP2 - inflection point of the second thermal unfolding (at a higher temperature)

k_D - interaction parameter

nanoDSF[®] - fluorimetric method based on intrinsic protein fluorescence

$P(r)$ – pair distance distribution function

ReFOLD – isothermal unfolding/refolding assay to assess protein aggregation

R_g – radius of gyration from SAXS

R_h - apparent protein hydrodynamic radius from DLS

RMY - relative monomer yield after refolding

SAXS – small-angle X-ray scattering

SEC - size exclusion chromatography

SLS – static light scattering

STD-NMR – saturation transfer difference nuclear magnetic resonance

T_{agg} - protein aggregation onset temperature from DLS

ABSTRACT

Understanding the effects of additives on therapeutic protein stability is of paramount importance for obtaining stable formulations. In this work, we apply several high- and medium-throughput methods to study the physical stability of a model monoclonal antibody at pH 5.0 and 6.5 in the presence of sucrose, arginine hydrochloride and arginine glutamate. In low ionic strength buffer, the addition of salts reduces the antibody colloidal and thermal stability, attributed to screening of electrostatic interactions. The presence of glutamate ion in the arginine salt partially reduces the damaging effect of ionic strength increase. The addition of 280 mM sucrose shifts the thermal protein unfolding to a higher temperature. Arginine salts in the used concentration reduce the relative monomer yield after refolding from urea, while sucrose has a favorable effect on antibody refolding. In addition, we show 12-month long-term stability data and observe correlations between thermal protein stability, relative monomer yield after refolding and monomer loss during storage. The monomer loss during storage is related to protein aggregation and formation of subvisible particles in some of the formulations. This study shows that the effect of commonly used additives on the long-term antibody physical stability can be predicted using orthogonal biophysical measurements.

INTRODUCTION

One fundamental aim during the development of therapeutic proteins is finding formulations that provide sufficient protein stability during long-term storage. Some critical variables of these formulations are solution pH, ionic strength, and the presence of additives. The additives usually belong to the group of sugars, polyols, amino acids, or surfactants^{1,2}. Among these, sucrose is the most frequently used in marketed therapeutic protein formulations¹. From the amino acids, arginine is of considerable interest, as in some cases it can suppress protein aggregation or reduce the viscosity of highly concentrated protein solutions^{3,4}. Also, the use of different arginine salts is a topic of intense research since the arginine counterion can determine the effect on protein stability⁴⁻⁷.

Sucrose and arginine salts can affect the thermal protein unfolding and aggregation differently depending on the protein molecule. The presence of other buffer components, such as NaCl, which modify the ionic strength of the solution, can also influence the direction and the magnitude in which arginine salts impact protein physical stability^{5,8-11}. Especially arginine can have complex effects on the protein unfolding, aggregate formation and aggregate growth, depending on the conditions and the nature of its counter-ion^{7,12}. The concentration of the additive is also essential but limited by the target osmolality of the formulation that typically should be close to physiological¹³. Many of the studies with sucrose and arginine salts observe effects on protein stability that depend on the additive concentration^{5,8,9,11}. Often, 0.5-1 M of sucrose or arginine hydrochloride (ArgHCl) has a beneficial impact on protein stability^{8,14-17}, whereas for arginine glutamate (ArgGlu) the optimal working concentration is typically much lower, 50-200 mM^{5,6,18}. High concentrations of additives make the solutions hypertonic and thus unsuitable for therapeutic protein formulations that will be injected undiluted in patients. Therefore, it is essential to study the effect of additives on protein stability in concentrations realistic for medicinal products. Just as importantly, published work on the impact of additives on protein stability is often not supported by long-term stability data to confirm that an additive will have a stabilizing or destabilizing effect during storage at temperatures relevant for therapeutic proteins.

The effects of additives on protein physical stability can be studied with various biophysical methods that require different sample volume and analytical effort. There are different classifications of these methods, some of which are based on throughput¹⁹. However, there are not always well-defined borders that would classify a method as high- or medium-throughput. In general, a higher throughput is related to lower sample volume, shorter measurement time and a high potential for method automation. Based on these criteria, in our work, we would like to define as high-throughput methods all methods that require less than 100 μ L sample, less than a day to complete the measurements for many samples and that can be automated. This includes nanoDSF® and DLS performed on samples in multi-well plates. As medium-throughput methods, we define techniques that require larger sample volume, up to 1 mL, longer time and higher analytical effort, and less potential for automation. Such techniques in the presented work are SAXS and NMR. The ReFOLD assay, which we also employ, falls in between high- and medium-throughput since it requires small sample volumes, is performed in deep multi-well plates, could be automated, but requires a few days to complete in its current set-up.

In this work, we apply the high- and medium-throughput methods mentioned above to study the effect of three additives, 280 mM sucrose, 140 mM ArgHCl, and 70 mM ArgGlu on the physical

stability of a model monoclonal antibody at pH 5.0 and 6.5. We focus on the impact of the additives on the colloidal protein stability and the protein aggregation during refolding from urea. Finally, we perform long-term stability studies for 12 months at 4 °C and 25 °C to investigate if the quick biophysical characterization can foresee the effects of the additives on the protein long-term storage stability.

MATERIALS AND METHODS

Monoclonal antibodies and chemicals

The monoclonal antibody PPI13 used in this work is a human IgG1k with a molecular mass of 148.9 kDa and an isoelectric point around 9. In the near future, the primary protein sequence and additional information about PPI13 will be available in an online database (<https://pippi-data.kemi.dtu.dk/>). PPI13 was supplied in surfactant-free bulk solution with protein concentration 43 g/L. Size exclusion chromatography was used to check the purity of PPI13 in bulk and showed >97 % monomer relative monomer content. The bulk buffer was exchanged to 10 mM histidine/histidine hydrochloride with pH 5.0, 5.75 and 6.5 at 25 °C using extensive dialysis as described earlier²⁰. The absorption of PPI13 at 280 nm was measured with a Nanodrop 2000 UV spectrophotometer (Thermo Fisher Scientific, Wilmington, DE) and the protein concentration was calculated using the protein extinction coefficient. Stock solutions of the additives - sucrose, ArgHCl, ArgGlu, guanidinium hydrochloride (GuHCl) and NaCl - were prepared in the respective histidine buffer and spiked to the dialyzed protein solution. All chemicals were high purity grade and were purchased from Sigma Aldrich (Steinheim, Germany), VWR International (Darmstadt, Germany) or Fisher Scientific (Schwerte, Germany). Ultrapure water from an arium® system (Sartorius Lab Instruments GmbH, Goettingen, Germany) was used to prepare all solutions.

Long-term stability study

PPI13 samples with protein concentration of 5 g/L in the respective buffer (or buffer plus additive) were sterile filtered with a 0.22 µm cellulose acetate filter, aseptically filled into sterilized DIN2R glass type I vials (Mglass AG, Germany), crimped with FluroTec® coated rubber chlorobutyl stoppers (West Pharmaceutical Services, USA), and stored at 4 °C and 25 °C for the desired time. Three different vials were used for the analysis of each condition and time.

Dynamic light scattering (DLS)

Before DLS measurements, all samples were centrifuged at 10,000g for 10 minutes. Next, 10 µL of PPI13 solution with 5 g/L protein concentration, unless otherwise stated, were filled in a 1536 microwell plate (Aurora, Whitefish, USA). The plate was centrifuged at 2200 rpm for 2 minutes using a Heraeus Megafuge 40 centrifuge equipped with an M-20 well plate rotor (Thermo Fisher Scientific, Wilmington, USA). Each well was subsequently sealed with 5 µL silicon oil and the plate was centrifuged again. The samples were then measured on a DynaPro plate reader III (Wyatt Technology, Santa Barbara, USA) using 3 acquisitions of 3 seconds during a linear temperature ramp of 0.1 °C/min from 25 to 85 °C. The Dynamics V7.8 software was used to visualize the autocorrelation functions (ACF) and to apply cumulant analysis giving the mutual diffusion coefficient (D) and the polydispersity index (PDI). The apparent protein hydrodynamic radius (R_h) was calculated using the Stokes-Einstein

equation from the D and the sample viscosity. The sample viscosity was measured with a falling ball viscometer AMVn (Anton Paar GmbH, Ostfildern-Scharnhausen, Germany). The aggregation onset temperature (T_{agg}) was determined using the onset fit function of the Dynamics V7.8 software from the R_h increase during heating. To derive the interaction parameter k_D , PPI13 samples with different protein concentration (see the Results section) were filled in 1536 microwell plates as described above. The samples were then measured at 25 °C with 10 acquisitions of 5 seconds. The mutual diffusion coefficient D was calculated as described above and the following equation was used to extract k_D :

$$D=D_0(1+k_Dc)$$

where D_0 is the diffusion coefficient at infinite dilution and c is the protein concentration. All DLS measurements were performed in triplicates.

High-throughput Fluorimetric Analysis of Thermal Protein Unfolding with nanoDSF®

The thermal unfolding of 5 g/L PPI13 in different formulations was studied with nanoDSF^{®21,22}. The samples were filled in standard glass capillaries, the capillaries were sealed and placed in a Prometheus® NT.48 (NanoTemper Technologies, Munich, Germany). The device was used to linearly change the sample temperature from 25 to 100 °C with a ramp of 0.1 °C/min. During the temperature increase, the intrinsic protein fluorescence intensity at 330 nm and 350 nm was measured after excitation at 280 nm (± 10 nm). Simultaneously, the back-reflection intensity of a light beam that passes through the capillary was measured to detect protein aggregation/precipitation. The scattering signal was normalized to the baseline signal to obtain a value called "Excess Scattering". The fluorescence intensity ratio (FI350/FI330) was plotted versus temperature, and the first (IP1) and second (IP2) inflection points of the protein thermal unfolding curve were determined from the maxima of the first derivative using the PR.ThermControl V2.1 software (NanoTemper Technologies, Munich, Germany). The protein thermal unfolding curves and inflection points measured with nanoDSF typically agree well with the unfolding curves and melting temperatures obtained with techniques like differential scanning calorimetry and circular dichroism^{23,24}.

Isothermal unfolding and refolding with urea (ReFOLD assay)

The assay was performed as described earlier²⁰. Briefly, 50 μ L of 5 g/L PPI13 solution in the respective buffer (or buffer plus additive) were filled in Pierce™ microdialysis devices (3.5 kDa MWCO). The samples were dialyzed in a deep well-plate against 1.5 mL of 9 M urea dissolved in the respective formulation buffer (or buffer plus additive). The urea solution was changed after 4 and 8 hours and the dialysis continued for 24 hours in total. Next, the PPI13 samples in 9 M urea were dialyzed using the same procedure against 1.5 mL of the respective urea-free formulation buffer (or buffer plus additive). During dialysis, the deep well plate was agitated at 700 rpm with a Thermomixer Comfort (Eppendorf AG, Hamburg, Germany). Subsequently, the samples were collected from the dialysis devices, each sample was weighed on a microbalance and the respective urea-free formulation buffer was added to a final weight of 250 mg. Finally, the samples were centrifuged at 10,000g for 10 minutes, and the supernatant was used for further measurements.

Size exclusion chromatography (SEC)

A Dionex Summit 2 system equipped with a UVD170U UV/Vis detector (Thermo Fisher, Dreieich, Germany) was used to inject PPI13 samples on a TSKgel G3000SWxl, 7.8x300 mm, 5 μm column (Tosoh Bioscience, Tokyo, Japan). The mobile phase with pH 7.0 consisted of 100 mM potassium phosphate, 200 mM sodium chloride and 0.05 % w/v sodium azide. The elution of the samples was detected at 280 nm. The chromatograms were collected and integrated with Chromeleon V6.8 (Thermo Fisher, Dreieich, Germany). The relative monomer yield (RMY) of the protein after isothermal unfolding/refolding in urea was calculated after dividing the area of the monomer peak of the refolded sample by the area of the monomer peak of the sample before unfolding/refolding²⁰. The soluble protein yield after refolding was calculated by dividing the area of all protein peaks detected with SEC after refolding by the area of all protein peaks before refolding. The value is then multiplied by 100 to obtain the soluble protein yield as a percentage. The relative area of aggregates and the monomer recovery of PPI13 during long-term storage were calculated as earlier described²⁰. Briefly, the area of the monomer peak after storage was divided by the area of the monomer peak measured at the beginning of the stability study and multiplied by 100. Thus, the monomer recovery will account for monomer loss during storage both due to the formation of small soluble aggregate and subvisible particles. The relative area of aggregates in the SEC chromatogram was calculated as the area of the aggregate peaks was divided by the total area of all protein peaks in the chromatogram and multiplied by 100. Therefore, the relative area of aggregates represents the small aggregates as a fraction of the soluble protein that is observed during elution in the SEC experiment. The relative area of fragments was calculated in an analogical way to the relative area of the aggregates. Finally, the loss of soluble protein was calculated from the change in the summed area of all protein peaks (i.e. aggregates, monomer and fragments) after storage.

Flow imaging microscopy

The subvisible particles formed during long-term storage of PPI13 were measured with a FlowCAM® 8100 (Fluid Imaging Technologies, Inc., Scarborough, ME, USA) equipped with a 10x magnification cell (81 μm x 700 μm). Particle images were obtained using 150 μL sample volume, a flow rate of 0.15 mL/min, an auto image frame rate of 29 frames/second and a sampling time of 74 seconds. The particle identification settings were 3 μm distance to the nearest neighbor, particle segmentation thresholds of 13 and 10 for the dark and light pixels respectively. The particle size reported represents the equivalent spherical diameter (ESD). The data was collected and processed with the VisualSpreadsheet® 4.7.6 software.

Small-angle X-ray scattering (SAXS)

Data collection was performed at the P12 beamline at the Petra III storage ring (DESY, Hamburg DE)²⁵ (see Table S1 in the Supplementary data for experimental details). The radius of gyration (R_g) and the maximum dimension (D_{max}) of PPI13 were derived from the experimental data with the data analysis program PRIMUSqt from the ATSAS software suite^{26,27}. The protein molecular mass (M_m) was calculated from the Porod volume ($M_m = \text{Porod volume} \times 1.7$), because this determination does not depend on absolute scaling or protein concentration.

Nuclear magnetic resonance (NMR)

NMR samples were prepared by the addition of $^2\text{H}_2\text{O}$ to a final concentration of 5 % v/v in each protein formulation and transferred to 5 mm NMR tubes (Wilmad). Protein concentration was 50 μM . Titration experiments were performed by reconstitution of pre-measured freeze-dried aliquots of additive with the protein sample. All NMR experiments were acquired at 25 °C on a Bruker 800 MHz Avance III spectrometer equipped with 5 mm TCI cryoprobe and temperature control unit. At each point of the titration, a saturation transfer difference (STD) spectrum was acquired using a standard Bruker stddiffesgp.3 pulse sequence with 20 ms spin-lock filter to eliminate protein signals. The on- and off-resonance saturation frequencies were 0.175 ppm and 20 ppm, respectively, with saturation time of 2.0 s. STD spectra were obtained by subtraction of on-resonance spectrum from the off-resonance spectrum. STD-amplification factors were calculated as described elsewhere²⁸. Peak assignment and representative examples of the STD-NMR spectra can be found in the Supplementary data (Fig S1).

RESULTS AND DISCUSSION

Effect of pH, sucrose and arginine salts on the thermal unfolding and aggregation of PPI13

In the buffer chosen for the study, at low ionic strength, PPI13 shows two unfolding transitions detected by the change in the intrinsic protein fluorescence ratio (Fig 1a). These transitions correspond well to the temperatures of circular dichroism changes in the near-UV protein spectra (Fig S2). Increasing pH from 5.0 to 5.75 and then further to 6.5 shifts the inflection point of the first unfolding transition to a higher temperature, while the effect on the second inflection point is minimal. In buffer with pH 5.0, the protein aggregation onset temperature measured with dynamic light scattering is around 78 °C and the R_h does not become larger than 7-8 nm up to 85 °C (Fig 1b). Correspondingly, no formation of large aggregates is detected with nanoDSF[®] up to 100 °C (Fig 1c). The reason for this is that the aggregation detection method of nanoDSF[®] can detect only larger particles (see Ref.²³), which were not present in the solution as evident from the DLS measurements. At pH 6.5, the T_{agg} from DLS is slightly lower (76.7 °C), and the sample R_h and excess scattering rapidly increase which indicates the formation of large aggregates and precipitation (Figs 1b and 1c). At pH 5.75, the measured parameters for PPI13 with nanoDSF and DLS fall in between the values measured at pH 5.0 and pH 6.5. Such pH dependence of thermal unfolding and aggregation is already reported for several other monoclonal antibodies^{21,29-31}. We then focused on the effect of several additives on the stability of PPI13 at pH 5.0 and pH 6.5 since the protein behaves differently in these conditions concerning its thermal unfolding and aggregation.

The addition of 280 mM sucrose shifts the inflection points of the unfolding transitions and the aggregation onset to a slightly higher temperature independent of pH and without affecting the aggregate growth (Figs 1d and 1g) (for values see Table 1). The stabilization effect of sucrose is known and can be explained by preferential exclusion³⁰⁻³⁴.

Contrary to sucrose, the addition of 140 mM ArgHCl at pH 5.0 shifts the protein aggregation onset and the inflection points of both unfolding transitions to lower temperatures (Fig 1d) (Table 1). ArgGlu has a more complex effect on the stability of PPI13 at pH 5.0, reducing the aggregation onset temperature, but in most cases slightly increasing the temperature of both thermal unfolding inflection

points (Table 1). The addition of arginine salts causes the formation of larger protein aggregates at pH 5.0 (Figs 1e and 1f). At pH 6.5, 140 mM ArgHCl and 70 mM ArgGlu affect the T_{agg} , IP1 and IP2 of PPI13 in a similar direction but with a smaller magnitude compared to pH 5.0 (Table 1). The early onset of protein aggregation induced by ArgHCl at pH 5.0 (indicated by an arrow in Fig 1e) is not observed at pH 6.5. As the starting ionic strength of the buffers used here is very low, the addition of ionic compounds, such as arginine salts, is expected to screen the electrostatic repulsion between PPI13 molecules bearing overall positive charge at pH 5.0 and 6.5, and partially screen intramolecular Coulomb interactions, affecting both colloidal and thermal stability.

Our findings agree well with published data about the effect of ArgHCl on the thermal unfolding of some proteins^{9,35,36}. Here, we should note that the pH of the histidine buffer will change slightly during heating, but this pH change is the same regardless of the additive. Therefore, thermal denaturation techniques can still be used as a quick check to see whether an additive affects the thermal stability of a protein or not. The unfavourable effect of arginine salts on the aggregation onset temperature of PPI13 under low ionic strength conditions encouraged us to investigate further the reasons for reduced colloidal stability in more detail using isothermal techniques that are more suitable for studies on histidine-based formulations.

Effects of sucrose and arginine salts on the colloidal stability of PPI13

Dynamic light scattering was used to study the effect of the additives on the colloidal stability of PPI13. In 10 mM histidine buffer with pH 5.0 and pH 6.5, at low ionic strength, the mutual diffusion coefficient of the protein increases with an increase in protein concentration (Fig 2). The addition of 280 mM sucrose does not change the sign of this concentration dependence. However, when 140 mM ArgHCl or 70 mM ArgGlu is added, the mutual diffusion coefficient of the protein decreases with increasing protein concentration (Fig 2). This effect can be explained by the increase in ionic strength upon addition of the arginine salts, which leads to the screening of the electrostatic repulsion between the protein molecules³⁷. We also used the data in Fig 2 to derive the interaction parameter k_D of PPI13 in these formulations (Table 1). Here, we would like to make a note that the k_D values obtained at pH 6.5 without arginine salts could be overestimated due to the low ionic strength of the solution³⁸, but their sign should not be affected. To confirm the observations in Fig. 2, we used multi-well plate-based static light scattering method to measure second virial coefficients A_2 of PPI13 in the presence of the additives and found good agreement between k_D and A_2 (Figure S3) that is already reported earlier for other antibodies³⁹.

Based on the k_D and A_2 data, we could confirm that the addition of both arginine salts reduces the repulsive protein interactions, thus reducing the colloidal stability of PPI13 which corresponds well with the lower aggregation onset temperatures (Table 1) and the larger aggregate growth at pH 5.0 (Figs 1e and 1f). This effect can be attributed to an increase in the ionic strength of the solution upon addition of these salts. Sucrose (280 mM), which does not change the ionic strength, has a much smaller effect on the k_D and A_2 of PPI13 compared to the arginine salts (Tables 1 and S2).

Effects of pH, sucrose and arginine salts on PPI13 detected with SAXS

The $P(r)$ functions of PPI13 have a double peak in all conditions tested, which is characteristic for multidomain proteins like monoclonal antibodies (Figs 3a and 3b). The $P(r)$ function of the protein

in 10 mM histidine with pH 5.0 and 6.5 without additives exhibits only a slightly different peak shape, meaning that the difference in pH between these two conditions probably has a minor effect on the conformation/structure of PPI13 (Figs 3a and 3b). Such structural differences were not detectable with near-UV circular dichroism (data not shown). However, at pH 5.0 the first thermal unfolding transition of PPI13 is at significantly lower temperatures compared to pH 6.5, indicating lower conformational stability (Fig 1a). Increasing the PPI13 concentration from approximately 2 g/L to 7 g/L at pH 5.0 leads to a small decrease in D_{max} from 15.2 to 14.0 nm and does not change the protein molecular mass which is in good agreement with the expected value for the monomeric protein (Figs 3c and 3e). When the PPI13 concentration is increased from approximately 2 g/L to 7 g/L in 10 mM histidine buffer with pH 6.5 without additives, the D_{max} increases slightly from 15.5 to 16.4 nm, and the protein molecular mass also increases from 155 to 172 kDa (Figs 3d and 3f). Such an increase could be due to the presence of oligomers appearing at higher concentrations. Further support for this hypothesis is that dynamic and static light scattering indicated the formation of larger species at protein concentrations above 10 g/L. Here, we should note that between 1 and 10 g/L, the mutual diffusion coefficient of PPI13 from DLS changed linearly with protein concentration (Fig 2). Even if we assume that the change in the diffusion coefficient is due to mixed effects of transient interactions and weak oligomer formation, we will still be correct in our earlier statements that a more pronounced decrease in D with increasing protein concentration indicates lower colloidal stability. In addition to these observations, PPI13 showed pH-, buffer- and additive-dependent solubility problems when we tried to concentrate the protein above 20 g/L (data not shown). Such solubility problems occurred, for example, when we increased the ionic strength of the solution by addition of NaCl, or when we tried to dialyze the protein in other buffers like citrate or phosphate. The addition of 280 mM sucrose has minor effects on the $P(r)$ function, D_{max} and the molecular mass of PPI13 compared to no additive (Fig 3). Both arginine salts induce changes in the shape of the peak in the $P(r)$ function (Figs 3a and 3b). Moreover, the D_{max} and the M_m of PPI13 in the presence of arginine salts is higher comparing to the one without additives (Figs 3c, 3d, 3e and 3f), which points to the formation of protein oligomers. Contrary to the samples with no additive and with sucrose, the $P(r)$ function of PPI13 in the presence of ArgHCl and ArgGlu has a characteristic tail, which is also an indication of the presence of oligomers (Figs 3a and 3b). The small-angle X-ray scattering curves of all measured PPI13 samples can be found in the Supplementary data (Figs S4 and S5), and the corresponding parameters from the analysis are summarized in Table S3.

Arginine salts reduce the colloidal and thermal stability of PPI13 due to an increase in ionic strength

Looking for a better understanding of how the additives affect the stability of PPI13, we assessed the IP1, IP2, T_{agg} , k_D and A_2 parameters of PPI13 in GuHCl and NaCl solutions having the same molar concentration as the arginine salts used above (Table S2). Both 140 mM GuHCl and 140 mM NaCl cause PPI13 unfolding and aggregation at a lower temperature in a similar way to ArgHCl (Table S2). These results indicate that the negative impact of ArgHCl on PPI13 is due to an increase in ionic strength and subsequent reduction in the colloidal protein stability, rather than the Arg cation itself. Interestingly, 70 mM ArgGlu has a significantly less negative impact on the thermal protein unfolding and aggregation compared to 70 mM GuHCl or 70 mM NaCl, with the latter being the most damaging for both the colloidal and thermal stabilities (Table S2). We conclude that the increase in

ionic strength itself significantly reduces the physical stability of PPI13, however, the nature of ions in ArgGlu can partially offset this effect, and more so than in ArgHCl. This indicates once again the advantage of ArgGlu over ArgHCl. As a control, we measured the osmolarity of the solutions, as a proxy for the ionic strength. The osmolarity of the formulations with all salts tested corresponds to the expected osmolarity of strong binary electrolytes (Table S4), indicating that the ionic strength of the formulations including salts with the same molar concentration will be similar. Small differences from the expected osmolarity were observed in some cases, e.g. for arginine hydrochloride and guanidine hydrochloride. These differences could be due to the way of interaction of the additives with the protein⁴⁰.

Interaction of additives with PPI13

We used saturation transfer difference NMR (STD-NMR) spectroscopy to assess the interactions of sucrose and arginine salts with PPI13 at pH 5.0 and 6.5. Saturation difference amplification factors (AF^{STD}), which show increased value if the ligand spends a considerable amount of time in the proximity to the protein, were calculated and plotted as a function of additive concentration. The concentration dependencies of AF^{STD} of each additive, at the two pH values, are very similar (Fig 4). Saturation of AF^{STD} values as additive concentration was increased is not observed in any of the tested conditions, indicating that interactions of additives with PPI13 are generally weak and transient, with an estimated dissociation constant greater than 100 mM. However, we can see a difference in the interactions of ArgHCl and ArgGlu compared to sucrose. All AF^{STD} values for different sucrose protons reach approximately the same value, indicating that sucrose does not have a preferential orientation when it interacts with PPI-13, suggesting that the interaction is isotropic and unspecific. On per-molar concentration basis, the values of AF^{STD} for sucrose were also much weaker than some of the values displayed by ArgHCl or ArgGlu protons (Fig 4). The AF^{STD} values for different protons of ArgHCl and ArgGlu were much more varied, implying more anisotropic interactions and suggesting that these additives have clear preferred orientations for the transient binding. In both cases, Arg interacts with PPI13 through the side chain, as evident by increasing AF^{STD} along the sidechain, towards the positively charged end. In the case of ArgGlu, glutamate binds to PPI13 as well, through the negatively charged side chain. Together these data indicate preferential binding of arginine salts to PPI13, and ArgGlu producing stronger saturation transfer effect than ArgHCl, which suggests that in the presence of Glu arginine probably spends more time in bound state, then in the presence of Cl⁻. This fits with the earlier suggestions regarding the nature of synergistic effect in Arg-Glu mixtures.¹⁸ Transient binding of Arg and Glu with PPI13 is likely to neutralize the surface charges on the protein molecule, screening the overall repulsive interactions in this case, and decreasing its colloidal stability. This further supports the earlier observations that arginine salts reduce the aggregation onset temperatures, the interaction parameter k_D , and the second virial coefficient A_2 , when added to PPI13 in 10 mM histidine buffer. The saturation transfer data is also consistent with the preferential exclusion of sucrose as a dominant mechanism for PPI13 stabilization.

Effect of additives on the aggregation during refolding of PPI13

We recently presented an unfolding/refolding assay, named ReFOLD, that can be used to assess the aggregation of urea-induced partially unfolded protein species²⁰. We applied this assay to study whether the additives tested here suppress the aggregation of the partially unfolded protein at pH 5.0 and pH 6.5. The 9 M concentration of urea was selected since it causes significant perturbations in the protein structure as shown by the change in the circular dichroism protein spectra (Fig S6). Also, 280 mM sucrose, 140 mM ArgHCl and 70 mM ArgGlu can be dissolved in this urea concentration.

After isothermal unfolding and refolding of PPI13, there is a significant reduction in the monomer peak detected by size exclusion chromatography (Fig 5a). This decrease is due to protein aggregation during refolding from urea, which leads both to the formation of smaller aggregates that can be detected with SEC and to the formation of larger aggregates that are filtered by the SEC column. We reported earlier similar observations for two other monoclonal antibodies²⁰. We then calculated the relative monomer yield (RMY) and soluble protein yield after refolding and observed that these values were lowest when the refolding was performed at pH 5.0 in the presence of 140 mM ArgHCl or 70 mM ArgGlu (Fig 5b). This corresponds well with the detrimental effect of these salts on the colloidal stability of PPI13 when added to the 10 mM histidine buffer that has low ionic strength. The addition of 280 mM sucrose results in higher RMY and soluble protein yield at both pH 5.0 and pH 6.5 which agrees with the stabilizing effect of this sugar during thermal denaturation of PPI13 (Figs 5b and 5c). In addition, the mean values of RMY are slightly higher at pH 6.5 compared to their counterparts at pH 5.0. That concurs with the other stability-indicating parameters measured earlier at these pH values (Table 1). The soluble protein yield correlates well with the RMY, which indicates that most of the PPI13 monomer is lost after refolding due to the formation of larger aggregates that are too large to be detected with the SEC method. The near-UV CD spectra of the refolded PPI13 resembled the spectra of the native PPI13 in all formulation that we tested (Fig S6).

The results that arginine salts reduce the relative monomer yield after refolding from urea might appear surprising at first since arginine is often used at high concentrations (i.e. 0.5-1.0 M) to suppress aggregation during refolding⁴¹. However, the formulations of PPI13 present an interesting case. As we showed earlier, PPI13 has high colloidal stability at low ionic strength in 10 mM histidine with pH 5.0 or pH 6.5. The addition of salts in concentration 70-140 mM negatively affects the colloidal protein stability and reduces the repulsive protein-protein interactions as shown by the reduction in the interaction parameter k_D and the aggregation onset temperature (Tables 1 and S2). Published work shows that the protein-protein interactions are directly linked to the aggregation during refolding of some proteins^{17,42}. This reveals that the effects of additives on the protein colloidal stability should be carefully considered from case to case, taking into account the solution conditions, to have a better understanding why specific concentrations of some additives promote protein aggregation during heating and refolding from denaturants.

Effect of sucrose and arginine salts on the aggregation of PPI13 during long-term storage

The stability of PPI13 during long-term storage at 4 °C and 25 °C was assessed with size exclusion chromatography and flow imaging microscopy. PPI13 presents a case in which the amount of soluble aggregates detected by SEC remained constant or decreased marginally during storage

(Fig S7). These aggregates were present in the bulk solution, which has about nine-fold higher protein concentration than the 5 g/L we used in our stability studies. The observation with SEC that the amount of soluble aggregates in the samples does not increase after storage were confirmed with dynamic light scattering (data not shown). Future work can focus on the aggregation mechanism and type of aggregates formed by PPI13, and how the aggregation depends on protein concentration.

A decrease in the monomer recovery of PPI13 was observed after storage which indicated a loss of soluble protein probably due to the formation of larger aggregates that are filtered out by the SEC column (Fig 6). Further support for this hypothesis is that we also observed a loss of soluble protein that correlated well with the decrease in the monomer recovery (Fig 6). In general, the decrease in monomer recovery was more pronounced at pH 5.0 compared to pH 6.5, and during storage at 25 °C compared to 4 °C. The formulations including 280 mM sucrose showed the highest recovery at both storage temperatures and both at pH 5.0 and pH 6.5. Interestingly, the formulations with 70 mM ArgGlu had monomer recoveries close to 100 % at pH 6.5 but not at pH 5.0.

We also observed fragmentation and formation of fragments in some of the samples. All conditions contained approximately 0.1 % relative fragment content at the beginning of the stability study. After 12-month storage at 4 °C, this level increased to 0.2 % in all samples tested, regardless of pH and additives. After storage at 25 °C for 12 months, the relative fragment area increased from 0.1 % to approximately 1.2 % in all conditions with pH 6.5, without influence from the additives. When the protein was stored at pH 5.0 without additive or with 280 mM sucrose, the relative area of fragments was 1.5 % after 12 months at 25 °C. However, when the protein was stored in the presence of arginine salts at pH 5.0 we observed a slightly higher relative amount of fragments of approximately 2 %.

The monomer loss of PPI13 in some of the samples is a result of the formation of larger aggregates detected as subvisible particles with flow imaging microscopy (Fig 7). At pH 5.0, the two arginine salts induced the formation of the largest number of particles in all three size ranges. 280 mM sucrose reduced the number of particles formed at pH 5.0 compared to no additive. These results concur well with the monomer recovery in Fig 6a. At pH 6.5 the particle counts were very low independent of the presence of additives. The samples stored at 4 °C showed very low particle numbers at both pH 5.0 and pH 6.5, and no clear difference between effect of different additives could be observed (Fig S8). The loss of monomer in samples where no subvisible particles were detected remains an open question. We assume that this monomer loss is either due to the formation of particles with size in the analytical gap between flow imaging microscopy and SEC (i.e. in the submicrometric range).

Correlation between stability-indicating parameters and long-term stability

To conclude the study, we looked for correlations between the different biophysical parameters measured and the monomer recovery and particle numbers after long-term storage at 25 °C. The rankings from the first thermal unfolding inflection point and the relative monomer yield after refolding from urea showed the strongest correlation with long-term stability data (Fig S9). In general, some of the correlations (Fig S9 – A, B, C, D, E) are weak due to the low particle numbers and small differences between most of the formulations. This causes the points to cluster in a narrow range. The

least stable formulations during long-term storage were the two formulations where the protein unfolds at lower temperature and has the lowest aggregation onset temperature, the lowest relative monomer yield after refolding from urea, and a negative interaction parameter k_D . Sucrose in concentration of 280 mM increases the temperature of thermal unfolding and the relative monomer yield after refolding from urea at pH 5.0. This corresponds well to the stabilizing effect of sucrose observed during storage compared to no additive. Many of the formulations, e.g. at pH 6.5, exhibit high monomer recovery and low particle numbers independent of the presence of an additive. It remains an open question, whether a difference between these formulations would be seen after longer storage time, i.e. for 24 or 36 months. Here, we should note that although the strength of the correlations in Fig S9 differ, we observe a consensus between the stability-indicating techniques, and they were all useful for identifying the two PPI13 formulations that were least stable during long-term storage, i.e. the ones based on 10 mM histidine pH 5.0 including arginine salts. Taking a decision which protein formulations should (or should not) be selected for further development is easier in such cases due to the general agreement between the stability-indicating parameters.

An interesting observation is that in the long-term stability studies with PPI13 we did not detect an increase in the amount of soluble aggregates but found that the protein aggregates by forming large particles in the conditions providing lower conformational and colloidal stability. When the protein is refolded from 9 M urea using the ReFOLD assay, we observe substantial monomer loss but only a small increase in the soluble aggregates, identified as dimers (Fig 5a). For comparison, two other IgG1-type monoclonal antibodies, which we studied earlier, form much more soluble aggregates with various sizes after refolding from urea²⁰. Based on these results, it is tempting to speculate that the aggregation mechanisms of PPI13 during long-term storage and during refolding from urea could be similar.

CONCLUSION

In this work, we applied orthogonal high- and medium-throughput techniques to probe the effect of 280 mM sucrose, 140 mM ArgHCl and 70 mM ArgGlu on the stability of a monoclonal antibody named PPI13. We found good agreement between various parameters showing that, under low ionic strength conditions, sucrose stabilizes the protein, while arginine salts in this concentration reduce the colloidal protein stability at both pH 5.0 and pH 6.5. This reduction can be explained by the increase in ionic strength and the screening of electrostatic repulsion between the protein monomers, once ions from arginine salts bind to the surface of the protein, as evident by our STD-NMR experiments. We also performed long-term stability studies to validate the observations from the quick biophysical characterization. The two parameters that show the strongest correlation with the long-term stability data are the temperature of the first thermal unfolding inflection point and the relative monomer yield after isothermal refolding from urea. Formulations in which PPI13 unfolds at lower temperature and has low colloidal stability are the formulations in which a considerable amount of subvisible particles were formed after 12-month storage at 25 °C.

Our work is important in two aspects. First, it shows that PPI13 formulations where multiple biophysical techniques indicate low physical stability are also formulations in which the protein aggregates during long-term storage. And second, we show that whether arginine salts will inhibit or

promote aggregation is highly dependent on other solution parameters, such as the starting ionic strength of the solution. Although arginine can undoubtedly bring benefits in formulations where the short-ranged hydrophobic interactions are important (e.g. at high protein concentration, or where long-range electrostatic repulsions are already largely screened), arginine salts can have a detrimental effect on the protein colloidal stability in protein formulations where electrostatic repulsion is important for suppressing protein aggregation (e.g. in dilute protein solutions at low ionic strength).

ACKNOWLEDGEMENTS

This study was funded by a project part of the EU Horizon 2020 Research and Innovation program under the Marie Skłodowska-Curie grant agreement No 675074. The authors would like to acknowledge and thank Dr. Robin Curtis at Manchester Institute of Biotechnology (MIB) for helpful discussions and advice, and Matthew Cliff from the MIB NMR Facility for technical and experimental support. The synchrotron SAXS data was collected at beamline P12 operated by EMBL Hamburg at the PETRA III storage ring (DESY, Hamburg, Germany). We would like to thank Stefano Da Vela for the assistance in using the beamline.

REFERENCES

1. Włodarczyk SR, Custódio D, Jr AP, Monteiro G. Influence and effect of osmolytes in biopharmaceutical formulations. *Eur J Pharm Biopharm.* 2018;131:92-98. doi:10.1016/j.ejpb.2018.07.019
2. Hamada H, Arakawa T, Shiraki K. Effect of additives on protein aggregation. *Curr Pharm Biotechnol.* 2009;10(4):400-407. doi:10.2174/138920109788488941
3. Inoue N, Takai E, Arakawa T, Shiraki K. Specific Decrease in Solution Viscosity of Antibodies by Arginine for Therapeutic Formulations. *Mol Pharm.* 2014;11:1889-1896. doi:10.1021/mp5000218
4. Dear BJ, Hung JJ, Laber JR, et al. Enhancing Stability and Reducing Viscosity of a Monoclonal Antibody with Co-solutes by Weakening Protein-Protein Interactions. *J Pharm Sci.* March 2019. doi:10.1016/J.XPHS.2019.03.008
5. Kheddo P, Tracka M, Armer J, et al. The effect of arginine glutamate on the stability of monoclonal antibodies in solution. *Int J Pharm.* 2014;473(1-2):126-133. doi:10.1016/j.ijpharm.2014.06.053
6. Golovanov AP, Hautbergue GM, Wilson SA, Lian LY, Bank W, Sheffield S. A simple method for improving protein solubility and long-term stability. *J Am Chem Soc.* 2004;126(29):8933-8939. doi:10.1021/ja049297h
7. Zhang J, Frey V, Corcoran M, Zhang-Van Enk J, Subramony JA. Influence of Arginine Salts on the Thermal Stability and Aggregation Kinetics of Monoclonal Antibody: Dominant Role of Anions. *Mol Pharm.* 2016;13(10):3362-3369. doi:10.1021/acs.molpharmaceut.6b00255
8. Arakawa T, Maluf NK. The effects of allantoin, arginine and NaCl on thermal melting and aggregation of ribonuclease, bovine serum albumin and lysozyme. *Int J Biol Macromol.* 2018;107:1692-1696. doi:10.1016/j.ijbiomac.2017.10.034

9. Platts L, Falconer RJ. Controlling protein stability: Mechanisms revealed using formulations of arginine, glycine and guanidinium HCl with three globular proteins. *Int J Pharm.* 2015;486(1-2):131-135. doi:10.1016/j.ijpharm.2015.03.051
10. Baynes BM, Wang DIC, Trout BL. Role of Arginine in the Stabilization of Proteins against Aggregation. *Biochemistry.* 2005;44(14):4919-4925. doi:10.1021/bi047528r
11. Arakawa T, Kita Y, Ejima D, Tsumoto K, Fukada H. Aggregation Suppression of Proteins by Arginine During Thermal Unfolding. *Protein Pept Lett.* 2006;13(9):921-927. doi:10.2174/092986606778256171
12. Yoshizawa S, Arakawa T, Shiraki K. Thermal aggregation of human immunoglobulin G in arginine solutions: Contrasting effects of stabilizers and destabilizers. *Int J Biol Macromol.* 2017;104:650-655. doi:10.1016/j.ijbiomac.2017.06.085
13. Setnikar I, Paterlini MR. Osmotic pressure and tolerance of injectable solutions. *J Am Pharm Assoc Am Pharm Assoc (Baltim).* 1960;49:5-7. doi.org/10.1002/jps.3030490103
14. Krishnan S, Chi EY, Webb JN, et al. Aggregation of granulocyte colony stimulating factor under physiological conditions: Characterization and thermodynamic inhibition. *Biochemistry.* 2002;41(20):6422-6431. doi:10.1021/bi012006m
15. Soenderkaer S, Carpenter JF, Van De Weert M, Hansen LL, Flink J, Frokjaer S. Effects of sucrose on rFVIIa aggregation and methionine oxidation. *Eur J Pharm Sci.* 2004;21(5):597-606. doi:10.1016/j.ejps.2003.12.010
16. Chi EY, Krishnan S, Kendrick BS, Chang BS, Carpenter JF, Randolph TW. Roles of conformational stability and colloidal stability in the aggregation of recombinant human granulocyte colony-stimulating factor. *Protein Sci.* 2003;12(5):903-913. doi:10.1110/ps.0235703.mer
17. Ho JGS, Middelberg APJ. Estimating the potential refolding yield of recombinant proteins expressed as inclusion bodies. *Biotechnol Bioeng.* 2004;87(5):584-592. doi:10.1002/bit.20148
18. Shukla D, Trout BL. Understanding the Synergistic Effect of Arginine and Glutamic Acid Mixtures on Protein Solubility. *J Phys Chem B.* 2011;115(41):11831-11839. doi:10.1021/jp204462t
19. Samra H, He F. Advancements in high throughput biophysical technologies: Applications for characterization and screening during early formulation development of monoclonal antibodies. *Mol Pharm.* 2012;9(4):696-707.
20. Svilenov H, Winter G. The ReFOLD assay for protein formulation studies and prediction of protein aggregation during long-term storage. *Eur J Pharm Biopharm.* 2019;137:131-139. doi:10.1016/J.EJPB.2019.02.018
21. Wanner R, Breitsprecher D, Duhr S, Baaske P, Winter G. Thermo-Optical Protein Characterization for Straightforward Preformulation Development. *J Pharm Sci.* 2017;106(10):2955-2958. doi:10.1016/j.xphs.2017.06.002
22. Linke P, Amaning K, Maschberger M, et al. An Automated Microscale Thermophoresis Screening Approach for Fragment-Based Lead Discovery. *J Biomol Screen.* 2016;21(4):414-421. doi:10.1177/1087057115618347
23. Svilenov H, Winter G. Rapid sample-saving biophysical characterisation and long-term storage stability of liquid interferon alpha2a formulations: Is there a correlation? *Int J Pharm.* 2019;562. doi:10.1016/j.ijpharm.2019.03.025
24. Breitsprecher D, Glücklich N, Hawe A, Menzen T. Thermal Unfolding of Antibodies Comparison of nanoDSF and μ DSC for thermal stability assessment during biopharmaceutical formulation development. *Appl Note NT-PR-006, NanoTemper Technol GmbH.* 2016.
25. Blanchet CE, Spilotros A, Schwemmer F, et al. Versatile sample environments and automation for biological solution X-ray scattering experiments at the P12 beamline (PETRA III, DESY). *J*

- Appl Crystallogr.* 2015;48(2):431-443. doi:10.1107/S160057671500254X
26. Petoukhov M V., Franke D, Shkumatov A V., et al. New developments in the ATSAS program package for small-angle scattering data analysis. *J Appl Crystallogr.* 2012;45(2):342-350. doi:10.1107/S0021889812007662
 27. Franke D, Petoukhov M V., Konarev P V., et al. ATSAS 2.8: a comprehensive data analysis suite for small-angle scattering from macromolecular solutions. *J Appl Crystallogr.* 2017;50(4):1212-1225. doi:10.1107/S1600576717007786
 28. Viegas A, Manso J, Nobrega FL, et al. Saturation-transfer difference (STD) NMR: A simple and fast method for ligand screening and characterization of protein binding. *J Chem Educ.* 2011;88(7):990-994. doi:10.1021/ed101169t
 29. Svilenov H, Markoja U, Winter G. Isothermal chemical denaturation as a complementary tool to overcome limitations of thermal differential scanning fluorimetry in predicting physical stability of protein formulations. *Eur J Pharm Biopharm.* 2018;125:106-113. doi:10.1016/j.ejpb.2018.01.004
 30. Alekseychik L, Su C, Becker GW, Treuheit MJ, Razinkov VI. High-Throughput Screening and Stability Optimization of Anti-Streptavidin IgG1 and IgG2 Formulations. *J Biomol Screen.* 2014;19(9):1290-1301. doi:10.1177/1087057114542431
 31. He F, Hogan S, Latypov RF, Narhi LO, Razinkov VI. High throughput thermostability screening of monoclonal antibody formulations. *J Pharm Sci.* 2010;99(4):1707-1720. doi:10.1002/jps.21955
 32. Feeney J, Fisher GH, Ryan JW, et al. Stabilization of Protein Structure by Sugars. *Biochemistry.* 1982;21:6536-6544 doi.org/10.1021/bi00268a033
 33. Barnett G V., Razinkov VI, Kerwin BA, et al. Osmolyte Effects on Monoclonal Antibody Stability and Concentration-Dependent Protein Interactions with Water and Common Osmolytes. *J Phys Chem B.* 2016;120(13):3318-3330. doi:10.1021/acs.jpcc.6b00621
 34. Kim NA, Thapa R, Jeong SH. Preferential exclusion mechanism by carbohydrates on protein stabilization using thermodynamic evaluation. *Int J Biol Macromol.* 2018;109:311-322. doi:10.1016/J.IJBIOMAC.2017.12.089
 35. Goldberg DS, Bishop SM, Shah AU, Sathish HA. Formulation Development of Therapeutic Monoclonal Antibodies Using High-Throughput Fluorescence and Static Light Scattering Techniques: Role of Conformational and Colloidal Stability. *J Pharm Sci.* 2011;100(4):1306-1315. doi:10.1002/jps.22371
 36. Thakkar S V., Joshi SB, Jones ME, et al. Excipients Differentially Influence the Conformational Stability and Pretransition Dynamics of Two IgG1 Monoclonal Antibodies. *J Pharm Sci.* 2012;101(9):3062-3077. doi:10.1002/jps.23187
 37. Roberts D, Keeling R, Tracka M, et al. The Role of Electrostatics in Protein-Protein Interactions of a Monoclonal Antibody. *Mol Pharm.* 2014;11(7):2475-2489. doi:10.1021/mp5002334
 38. Sorret LL, DeWinter MA, Schwartz DK, Randolph TW. Challenges in Predicting Protein-Protein Interactions from Measurements of Molecular Diffusivity. *Biophys J.* 2016;111(9):1831-1842. doi:10.1016/j.bpj.2016.09.018
 39. Menzen T, Friess W. Temperature-Ramped Studies on the Aggregation, Unfolding, and Interaction of a Therapeutic Monoclonal Antibody. *J Pharm Sci.* 2014;103(2):445-455. doi:10.1002/JPS.23827
 40. Courtenay ES, Capp MW, Anderson CF, Record MT. Vapor Pressure Osmometry Studies of Osmolyte-Protein Interactions: Implications for the Action of Osmoprotectants in Vivo and for the Interpretation of "Osmotic Stress" Experiments in Vitro. *Biochemistry.* 2000;39(15):4455-4471. doi:10.1021/bi992887l

41. Tsumoto K, Umetsu M, Kumagai I, Ejima D, Philo JS, Arakawa T. Role of Arginine in Protein Refolding, Solubilization, and Purification. *Biotechnol Prog.* 2004;20(5):1301-1308. doi:10.1021/bp0498793
42. Ho JGS, Middelberg APJ, Ramage P, Kocher HP. The likelihood of aggregation during protein renaturation can be assessed using the second virial coefficient. *Protein Sci.* 2003;12(4):708-716. doi.org/10.1110/ps.0233703

FIGURE LEGENDS

Figure 1. Thermal protein unfolding of PPI13 at different pH (**a**) and effect of additives on the thermal unfolding at pH 5.0 (**d**) and pH 6.5 (**g**). Effect of temperature on the apparent hydrodynamic radius R_h of PPI13 at different pH (**b**) and effect of additives on R_h during heating at pH 5.0 (**e**) and pH 6.5 (**h**). Effect of temperature on the excess scattering of PPI13 formulations at different pH (**c**) and effect of additives on the excess scattering during heating at pH 5.0 (**f**) and pH 6.5 (**i**). In A, C, D, F, G, and I the datapoint density is reduced to improve clarity. The concentration of PPI13 is 5 g/L in all samples.

Figure 2. Concentration dependence of the mutual diffusion coefficient of PPI13 at pH 5.0 (**a**) and pH 6.5 (**b**) in presence of no additive (squares), 280 mM sucrose (circles), 140 mM ArgHCl (triangles up) and 70 mM ArgGlu (triangles down). The data is overlay of triplicates. The lines present a linear fit to the points.

Figure 3. Overview of the results obtained with SAXS: $P(r)$ functions of PPI13 at pH 5.0 (**a**) and pH 6.5 (**b**), D_{max} at pH 5.0 (**c**) and pH 6.5 (**d**), M_m at pH 5.0 (**e**) and pH 6.5 (**f**).

Figure 4. Protein-additive saturation transfer amplification factors (AF^{STD}) measured for individual atoms of various additives added to PPI13 at pH 5.0 (left column) and 6.5 (right column), for sucrose (**a, b**), ArgHCl (**c, d**) and ArgGlu (**e, f**). The labels below the graphs specify individual atoms for which AF^{STD} was measured, and the insets show chemical structure of the additive molecules used with matching labelling of the atoms.

Figure 5. (**a**) SEC chromatogram of native and refolded PPI13 in 10 mM histidine pH 5.0. In a separate experiment, the peak at 14.2 minutes was identified as a dimer using SEC coupled to multi-angle light scattering (data not shown). Relative monomer yield and soluble protein yield of PPI13 when the protein is refolded from 9 M urea at pH 5.0 (**b**) and pH 6.5 (**c**) with no additive, 280 mM

sucrose, 140 mM ArgHCl or 70 mM ArgGlu. The values in B and C are mean of triplicates, the error bar is the standard deviation.

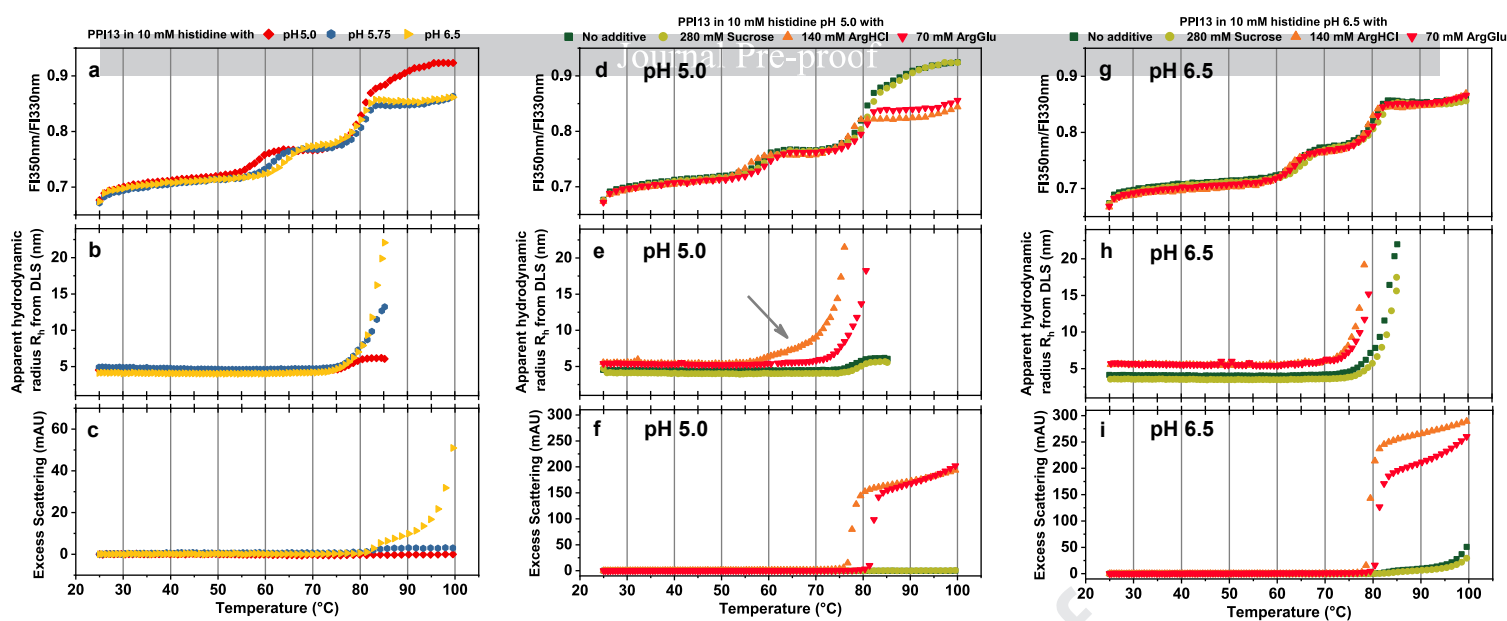
Figure 6. Effect of additives on the monomer recovery and loss of soluble PPI13 from size exclusion chromatography after 12 months of storage. (a) storage at 25 °C at pH 5.0, (b) storage at 25 °C at pH 6.5, (c) storage at 4 °C at pH 5.0, (d) storage at 4 °C at pH 6.5;

Figure 7. Effect of pH and additives on the subvisible particles of PPI13 measured during storage for 12 months at 25 °C

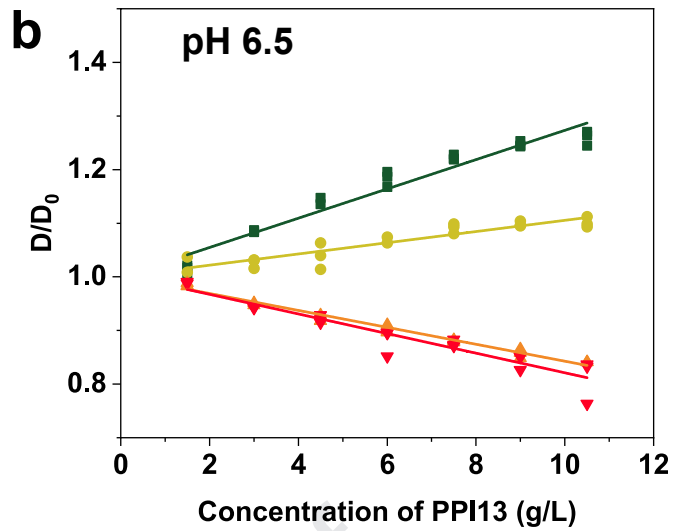
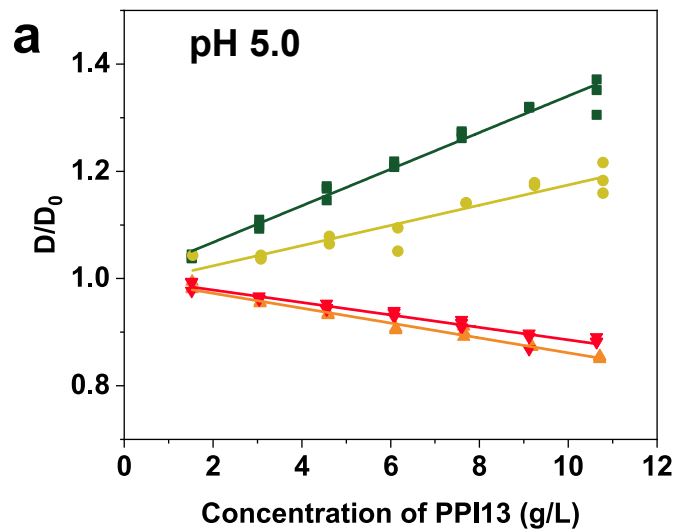
Journal Pre-proof

Table 1. Stability-indicating parameters of PPI13 in 10 mM histidine buffer with pH 5.0 and pH 6.5 in presence of different additives. The values are mean of triplicates, the error presents the standard deviation.

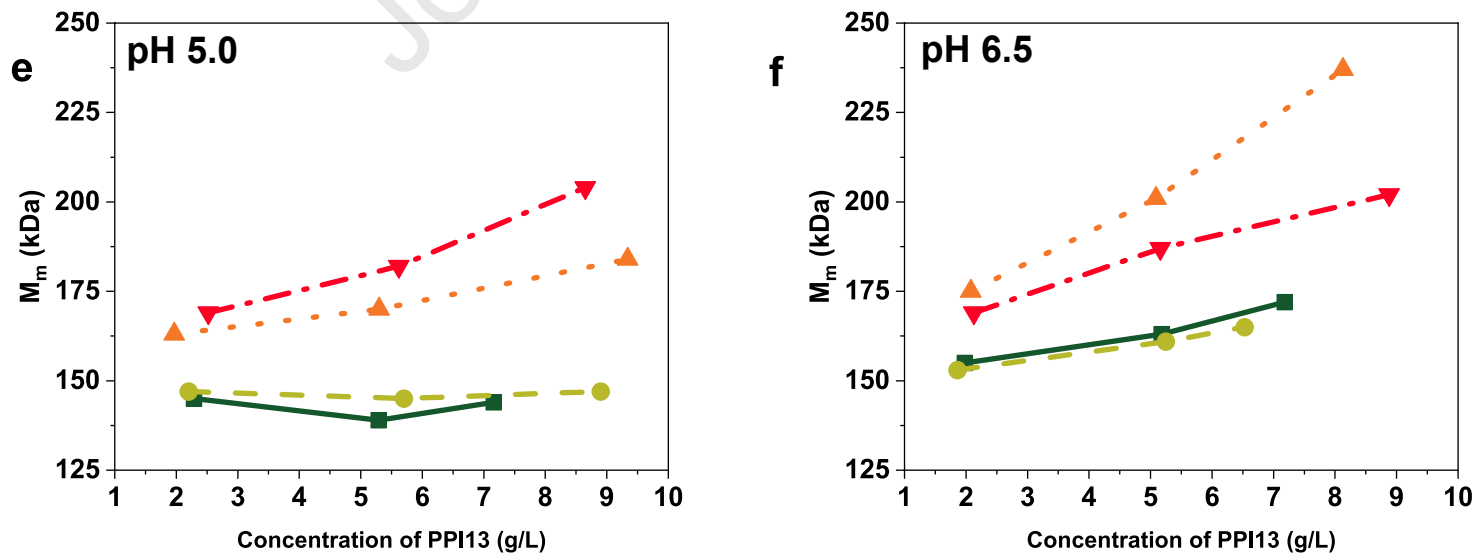
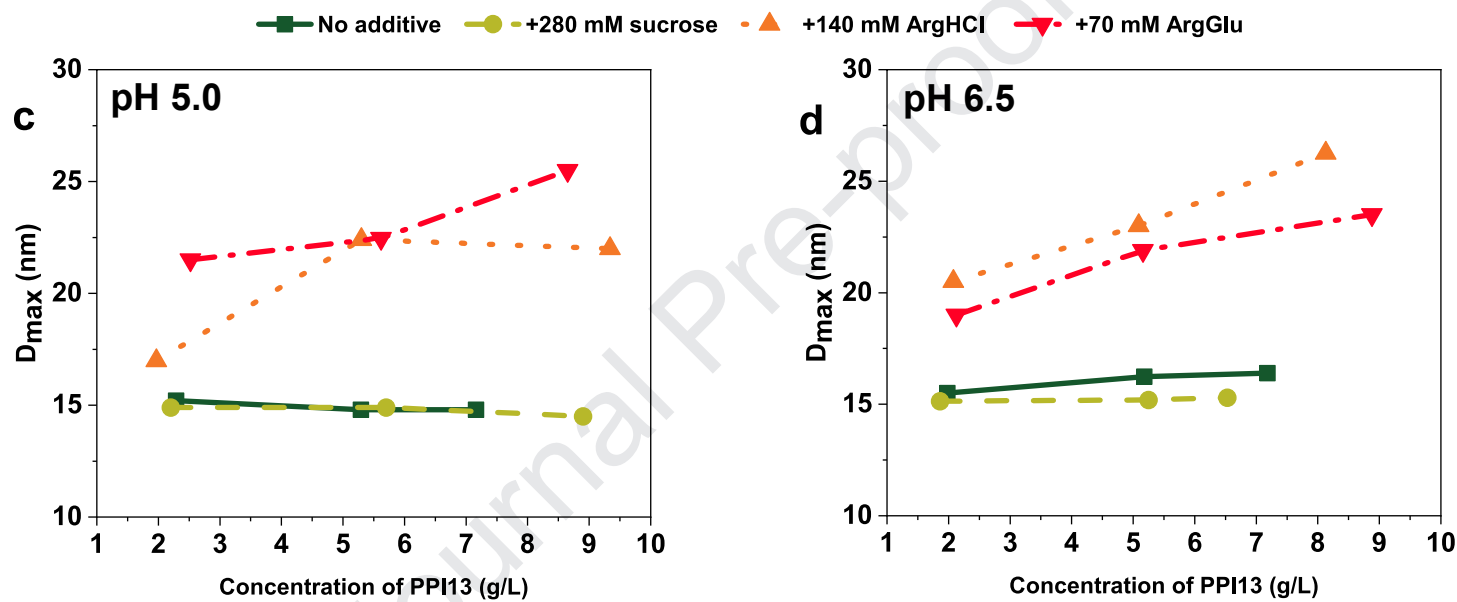
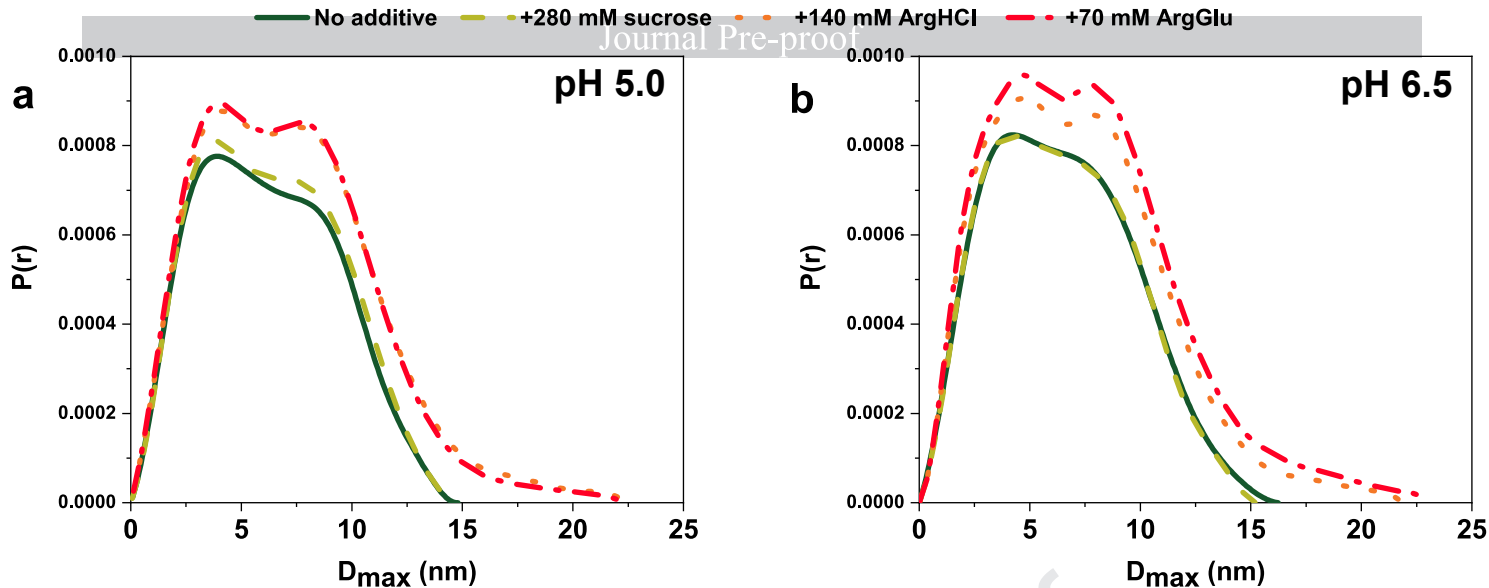
	Additive	From nanoDSF®		From DLS		
		IP1, °C	IP2, °C	T_{agg} , °C	k_D (mL/g)	$(\times 10^{-07} D_0 \text{ cm}^2/\text{s})$
pH 5.0	No	58.20 ± 0.05	80.17 ± 0.07	78.1 ± 0.3	34.2 ± 3.8	4.69 ± 0.08
	280 mM Sucrose	59.32 ± 0.06	81.04 ± 0.05	78.9 ± 0.1	17.1 ± 2.1	4.15 ± 0.09
	140 mM ArgHCl	55.43 ± 0.06	76.99 ± 0.03	60.8 ± 0.9	-13.9 ± 0.3	4.48 ± 0.02
	70 mM ArgGlu	59.70 ± 0.09	80.37 ± 0.01	73.3 ± 0.2	-11.1 ± 0.9	4.48 ± 0.03
pH 6.5	No	64.33 ± 0.10	80.11 ± 0.04	76.7 ± 0.4	27.3 ± 1.5	5.01 ± 0.03
	280 mM Sucrose	65.86 ± 0.11	81.24 ± 0.03	77.4 ± 0.4	10.7 ± 0.8	4.62 ± 0.04
	140 mM ArgHCl	62.25 ± 0.06	78.97 ± 0.04	73.3 ± 0.5	-15.7 ± 0.7	4.55 ± 0.02
	70 mM ArgGlu	63.84 ± 0.02	80.36 ± 0.01	74.1 ± 0.5	-16.6 ± 1.8	4.46 ± 0.06



Journal Pre-proof



Journal Pre-proof



pH 5.0

pH 6.5

